PHYSICAL REVIEW B VOLUME 15, NUMBER 4 15 FEBRUARY 1977

Optical properties of aggregated metal systems: Interband transitions*

J. P. Marton and B. D. Jordan
Department of Engineering Physics and The Institute for Materials Research, McMaster University, Hamilton, Ontario, L8S 4M1, Canada
(Received 23 September 1976)

In previous publications we reported on the optical properties of aggregated metal systems, where the metal particles were assumed to be free-electron type with damping, and where they were assumed to be dispersed in a dielectric medium with a varying index of refraction. The main results were the shift of bulk and surface plasma frequencies with aggregation density and the appearance of an extra resonance, called the optical conduction resonance (OCR), on the low-energy side of the plasma frequency. The OCR was shown to be a transverse collective mode of the free electrons in the aggregates which could be excited by incident light. In the present work the effects of electronic interband transitions on the free-electron OCR and the free-electron plasma frequencies are examined. Important new results are obtained including frequency shifts and splitting of the OCR absorption peak and the loss function by interband transitions. These results are used in the analysis of the dielectric functions of some real metals in aggregated form.

I. INTRODUCTION

It is generally accepted that if metal particles in an aggregated metal system are much smaller than the wavelength of light, and are roughly spherical, then their response to the incident radiation may be approximated by considering them to be dipoles. For a three-dimensional system this approximation leads to the familiar Maxwell-Garnett (MG) expression[1]

$$\frac{\tilde{\xi}(\omega)-n^2}{\tilde{\xi}(\omega)+2n^2}=\frac{q[\tilde{\epsilon}(\omega)-n^2]}{\tilde{\epsilon}(\omega)+2n^2}\,, \tag{1}$$

where $\tilde{\xi}(\omega)=\xi_1(\omega)+i\xi_2(\omega)$ is the complex dielectric function of the aggregated system, $\tilde{\epsilon}(\omega)=\epsilon_1(\omega)+i\epsilon_2(\omega)$ is the complex dielectric function of the metal aggregates, n is the index of refraction of the dielectric medium in which the metal particles are dispersed, and q is the volume fraction of the metal in the system. For a two-dimensional aggregated system, such as an aggregated thin metal film, or a rough metal surface the dipole approximation leads to a pair of equations[2] describing the optical properties parallel and perpendicular to the system. These have been called the generalized MG equations. They are given for $n=1$ by

$$\frac{\tilde{\xi}_{\parallel}(\omega)-1}{\tilde{\xi}_{\parallel}(\omega)+(4\pi-a)/a}=q\,\frac{\tilde{\epsilon}(\omega)-1}{\tilde{\epsilon}(\omega)+(4\pi-a)/a}\,, \tag{2a}$$

$$\frac{\tilde{\xi}_{\perp}(\omega)-1}{\tilde{\xi}_{\perp}(\omega)+a/(4\pi-a)}=q\,\frac{\tilde{\epsilon}(\omega)-1}{\tilde{\epsilon}(\omega)+a/(4\pi-a)}\,, \tag{2b}$$

where $\tilde{\xi}_{\parallel}(\omega)$ and $\tilde{\xi}_{\perp}(\omega)$ are, respectively, the parallel and perpendicular components of the dielectric function, and a is a constant whose value depends on the configuration of the dipoles chosen. The latter has been found[3] to describe the anisotropic nature of aggregated films and surfaces correctly.

The polarizability of metal particles, which is included in the dielectric function $\tilde{\epsilon}(\omega)$ had been assumed in our previous work[4] to be due entirely to free electrons. In this approximation, the real and imaginary parts of $\tilde{\epsilon}$ are given by

$$\epsilon_1(\omega)=1-\omega_{pf}^2\tau^2/(1+\omega^2\tau^2)\,, \tag{3a}$$

$$\epsilon_2(\omega)=\omega_{pf}^2\tau/\omega(1+\omega^2\tau^2)\,, \tag{3b}$$

where ω_{pf} is the free-electron plasma frequency $\omega_{pf}=(4\pi Ne^2/m^*)^{1/2}$ and τ is the relaxation time of the free electrons. N and m^* are, respectively, the number density and the effective mass of the free electrons. The aggregated system was shown in previous work[4] to exhibit a resonance absorption called the optical-conduction resonance (OCR), and the bulk-plasma frequency was found to be shifted from that of the bulk-metal value. Other quantities of interest, i.e., the optical conductivity, the surface plasma, and loss functions for the system were also analyzed.

In a later treatment,[5] the optical functions of the aggregated system were reexamined by allowing the electronic relaxation time to vary from the low-damping ($\omega_{pf}\tau\gg1$) to the high-damping ($\omega_{pf}\tau\lesssim1$) limit, and by allowing the refractive index of the matrix material n to change. This treatment yielded results which could be compared with experimental data on real metals. However, comparison was possible for long optical wavelengths and for some alkali metals only because at shorter wavelengths and for other metals, interband transitions would have changed the value of the dielectric function substantially from the free-electron value.

In order to describe the optics of real metals, the complete dielectric function is needed, which includes the free-electron part as well as the

full specification of electronic interband transitions, viz.,

$$\tilde{\epsilon}(\omega) = \tilde{\epsilon}^{(f)}(\omega) + \tilde{\epsilon}^{(i)}(\omega) , \tag{4}$$

where $\tilde{\epsilon}^{(f)}(\omega)$ is given by Eq. (3) and where $\tilde{\epsilon}^{(i)}(\omega)$ is given by

$$\tilde{\epsilon}^{(i)}(\omega) = \omega_{pf}^2 \sum_{j \neq 0} \frac{f_{j0}}{\omega_{j0}^2 - \omega^2 - i\omega\gamma_j} . \tag{5}$$

Here the symbols have their usual meaning, j refers to the jth excited level, f_{j0} is the oscillator strength of transition from the conduction band to the jth level, $1/\gamma_j$ is the relaxation time of the transition, and $\hbar\omega_{j0} = E_j - E_0$.

In the present work, the optical functions of aggregated metal systems are analyzed where the dielectric function of the metal particles is taken to contain both the free-electron part and the interband part with their respective relaxation times. The treatment will be shown to yield results that give a close description of real metal aggregated systems.

II. THEORY

To derive the optical functions of the aggregated system, its dielectric function $\tilde{\xi}(\omega)$ must be expressed in terms of the dielectric function of the metal aggregates $\tilde{\epsilon}(\omega)$, the metal volume fraction q, and the refractive index n of the dielectric matrix from Eq. (1). If we consider the case of $n = 1$ for simplicity, we get

$$\tilde{\xi}(\omega) = \frac{a\tilde{\epsilon}(\omega) + b}{c\tilde{\epsilon}(\omega) + d} \equiv \frac{f(\tilde{\epsilon})}{g(\tilde{\epsilon})} , \tag{6}$$

where

$$a = 1 + 2q, \quad b = 2(1 - q), \quad c = 1 - q, \quad d = 2 + q .$$

The real and imaginary parts of $\tilde{\xi}(\omega)$ are, respectively,

$$\xi_1(\omega) = \frac{f(\epsilon_1)g(\epsilon_1) + ac\epsilon_2^2}{g(\tilde{\epsilon})g^*(\tilde{\epsilon})} , \tag{7a}$$

$$\xi_2(\omega) = \frac{9q\epsilon_2}{g(\tilde{\epsilon})g^*(\tilde{\epsilon})} , \tag{7b}$$

where $f(\epsilon_1) = a\epsilon_1(\omega) + b$, $g(\epsilon_1) = c\epsilon_1(\omega) + d$, and g^* is the complex conjugate of g.

The inverse of Eq. (6) is useful for the bulk-plasma loss function. $\tilde{\xi}^{-1}(\omega)$ is given by

$$\tilde{\xi}^{-1}(\omega) = g(\tilde{\epsilon})/f(\tilde{\epsilon}) , \tag{8}$$

so the bulk loss function $L(\omega) = -\mathrm{Im}[\tilde{\xi}^{-1}(\omega)]$ is

$$L(\omega) = 9q\epsilon_2/f(\tilde{\epsilon})f^*(\tilde{\epsilon}) , \tag{9}$$

where f^* is the complex conjugate of f. If we now write the denominators

$$f(\tilde{\epsilon})f^*(\tilde{\epsilon}) = (1 + 2q)^2[(\epsilon_1 + b/a)^2 + \epsilon_2^2] , \tag{10}$$

$$g(\tilde{\epsilon})g^*(\tilde{\epsilon}) = (1 - q)^2[(\epsilon_1 + d/c)^2 + \epsilon_2^2] , \tag{11}$$

then it is apparent that Eqs. (7) and (9) are resonance functions, with ϵ_2^2 acting as the damping term. For small values of ϵ_2^2, resonance occurs at those ω values where

$$\epsilon_1(\omega) = -b/a = -2(1 - q)/(1 + 2q) \tag{12}$$

for the loss function in Eq. (9), and where

$$\epsilon_1(\omega) = -d/c = -(2 + q)/(1 - q) \tag{13}$$

for the dielectric constants in Eq. (7).

The specification of condition for bulk-plasma resonance and conduction resonance by Eqs. (12) and (13), respectively, is more useful for our present purpose than those used in our previous analysis.[4] We should briefly mention here that for $q = 1$, which represents the bulk metal, we get back naturally the conditions for bulk-plasma resonance, which is $\epsilon_1 = 0$, and for conduction resonance which is $\epsilon_1 = -\infty$ (the latter is the condition for dc conduction). If the damping term ϵ_2^2 is not negligible in the frequency range where resonance occurs, then conditions (12) and (13) no longer hold. For example, if ϵ_2 changes rapidly in the resonance region due to interband processes the resonance conditions for the aggregated system become, respectively,

$$\epsilon_1(\omega) = -\frac{b}{a} + \epsilon_2(\omega)\left(\frac{d\epsilon_2}{d\omega} \Big/ \frac{d\epsilon_1}{d\omega}\right) , \tag{14}$$

$$\epsilon_1(\omega) = -\frac{d}{c} + \epsilon_2(\omega)\left(\frac{d\epsilon_2}{d\omega} \Big/ \frac{d\epsilon_1}{d\omega}\right) . \tag{15}$$

This leads to a shift of frequency from the case of small ϵ_2 and to a skewed shape of the resonance curve. Such shifts in frequency of the bulk-plasma loss function from the free-electron value, caused by interband transitions, are well known[6] for some bulk metals.

Because our current interest is to analyze the effects of interband transitions on the OCR and plasma resonances of aggregated systems, we concentrate on the magnitude and spectrum of ϵ_2 in the range of frequencies where these resonances would otherwise take place when interband transitions are absent. In the latter case, we would naturally have $\epsilon_1^{(i)}(\omega) = \epsilon_2^{(i)}(\omega) = 0$ in the expressions

$$\epsilon_1(\omega) = \epsilon_1^{(f)}(\omega) + \epsilon_1^{(i)}(\omega) \tag{16a}$$

and

$$\epsilon_2(\omega) = \epsilon_2^{(f)}(\omega) + \epsilon_2^{(i)}(\omega) , \tag{16b}$$

where $\tilde{\epsilon}(\omega) = \epsilon_1(\omega) + i\epsilon_2(\omega)$ as before, and where $\epsilon_1^{(f)}$ and $\epsilon_2^{(f)}$ are the free-electron functions, given by Eq. (3). As it is well known[4] from previous

work, in the free-electron case $\epsilon_2(\omega)$ in Eq. (16b) is quite small in the OCR and plasma-resonance frequency region, so the conditions for resonance are simply Eqs. (12) and (13).

In order to introduce interband terms into the dielectric function, we can use a damped Lorentzian oscillator, rather than the proper interband term given by Eq. (5). The reason for this is twofold. First we are seeking the general features of the resulting optical functions only, and second, it would be difficult to write analytical expressions for the interband part of the dielectric function for even the simplest of metals, using Eq. (5). Our choice then is to use the oscillator

$$\epsilon^{(i)}(\omega) = \omega_{pf}^2 f/(\omega_0^2 - \omega^2 - i\omega\gamma) , \tag{17}$$

where ω_{pf} is the free-electron bulk-plasma-resonance frequency, f is the oscillator strength, ω_0 is the oscillator-resonance frequency, and γ^{-1} is the relaxation time. The real and imaginary parts of Eq. (17) are

$$\epsilon_1^{(i)}(\omega) = \frac{\omega_{pf}^2 f(\omega_0^2 - \omega^2)}{(\omega_0^2 - \omega^2)^2 + \omega^2\gamma^2} , \tag{18a}$$

$$\epsilon_2^{(i)}(\omega) = \frac{\omega_{pf}^2 f\omega\gamma}{(\omega_0^2 - \omega^2)^2 + \omega^2\gamma^2} . \tag{18b}$$

The complete dielectric function to be used for the analysis then is

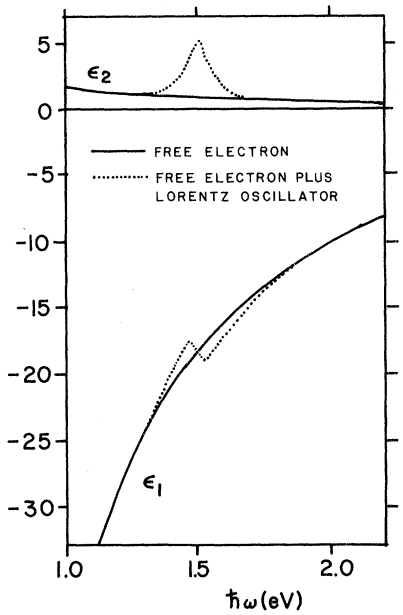

FIG. 1. Dielectric function of a hypothetical metal composed of a free-electron part with $\hbar\omega_{pf} = 6.6$ eV, $\tau = 2.6\times10^{-14}$ sec, and a damped Lorentz-oscillator part with $\hbar\omega_0 = 1.5$ eV, $\gamma^{-1} = 10^{-14}$ sec, $f = 0.01$, according to Eq. (19). The free-electron part is typical of a single-valent metal at room temperature.

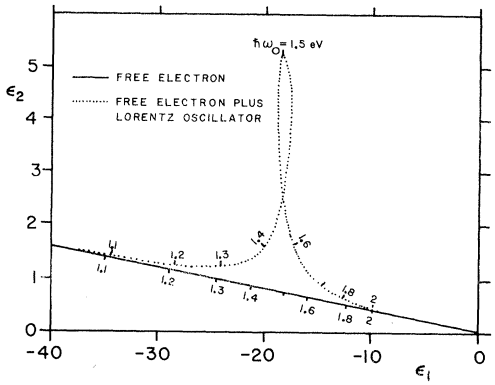

FIG. 2. Dielectric function shown in Fig. 1 replotted on the (ϵ_1, ϵ_2) Cartesian plane. This form of plotting enables the function to be easily analyzed at various q values by the MG coordinate transformation used in earlier work. The loop indicates an interband transition, and the area it encloses is inversely proportional to γ.

$$\epsilon_1(\omega) = 1 - \frac{\omega_{pf}^2\tau^2}{1+\omega^2\tau^2} + \frac{\omega_{pf}^2 f(\omega_0^2 - \omega^2)}{(\omega_0^2 - \omega^2)^2 + \omega^2\gamma^2} , \tag{19a}$$

$$\epsilon_2(\omega) = \frac{\omega_{pf}^2\tau}{\omega(1+\omega^2\tau^2)} + \frac{\omega_{pf}^2 f\omega\gamma}{(\omega_0^2 - \omega^2)^2 + \omega^2\gamma^2} , \tag{19b}$$

where the symbols have their usual meanings. The analysis consists of the evaluation of functions $\epsilon_1(\omega)$, $\epsilon_2(\omega)$, $\xi_1(\omega)$, $\xi_2(\omega)$, and $L(\omega)$ given by Eqs. (19a), (19b), (7a), (7b), and (9), respectively, for various values of ω_0 relative to ω_{pf}. The parameters used for the free-electron part of the dielectric function are the same as those used in our previous work,[4] i.e., we chose $\hbar\omega_{pf} = 6.6$ eV and $\tau = 2.6\times10^{-14}$ sec. This represents a hypothetical monovalent metal typical of good conductors at room temperature.

A typical plot of our dielectric function $\tilde{\epsilon}(\omega)$ composed of a free electron and a damped Lorentz-oscillator part, using Eq. (19), is given in Fig. 1. The same function is replotted on the (ϵ_1, ϵ_2) plane in Fig. 2. The latter form of plotting has been used in previous work[4,5] to visualize, and to graphically analyze, the features of the aggregated dielectric function $\tilde{\xi}(\omega)$ at particular aggregation parameter q, by superimposing the MG transformed curvilinear (ξ_1, ξ_2) coordinate system on the (ϵ_1, ϵ_2) Cartesian plane. This method of analysis was found to be particularly useful to visualize the optical-conduction resonance (OCR) for free-electron metals and to evaluate its properties as a function of the variables that control it. Here we follow a similar procedure in order to learn the effect of the position and strength of the Lorentzian oscillator on the free-electron OCR and plasma-resonance features of aggregated systems at different q values.

III. RESULTS

A very simple and useful qualitative analysis of the OCR and plasma resonance is possible using the representation of the dielectric function $\tilde{\epsilon}(\omega)$ on the (ϵ_1, ϵ_2) plane as shown in Fig. 2, if the resonance conditions Eqs. (10), (11), (14), and (15) are clearly understood. As was mentioned above, resonance occurs where ff^* and gg^* are minimum, which take place at the ω value for which $\epsilon_1(\omega)$ is equal to the right-hand side of Eq. (14) or (15) for a given value of q. Therefore, for a given value of q, we have two points on the ϵ_1 axis according to Eqs. (14) and (15), one for OCR and the other for plasma resonance. Now an inspection of Eqs. (10) and (11) shows that the shortest vectors connecting these points on the ϵ_1 axis with the $\tilde{\epsilon}(\omega)$ curve represent the minimum of ff^* and gg^*, thus the vectors point to the OCR and bulk-plasma-resonance points on the $\tilde{\epsilon}(\omega)$ curve. The idea is illustrated in Fig. 3 where we show the situation for $q = 0.3$ using the same $\tilde{\epsilon}(\omega)$ curve as that appearing in Fig. 2, except with $\hbar\omega_0 = 4$ eV.

It is apparent from Fig. 3 that, for the particular example chosen, the presence of the interband transition does not effect either the free-electron OCR or the free-electron plasma resonance. If we now move the interband frequency ω_0 to different values, in a sequence of moves as shown in Fig. 4, we see that as ω_0 approaches the free-electron OCR frequency ω'_{Rf} from above, the latter shifts to lower values. Also, in the region where ω_0 is approximately equal the free-electron OCR frequency, the OCR splits into a doublet. Further decreases of ω_0 restore ω'_R to the free-electron OCR frequency again. Similarly, if we move ω_0 in Fig. 3 to higher values, the frequency ω''_R of the bulk-loss function of the aggregated system first increases, then splits and finally it settles back to a free-electron value ω''_{Rf}. The doublet occurs in the region where ω_0 is approximately equal to the free-electron bulk-loss function frequency.

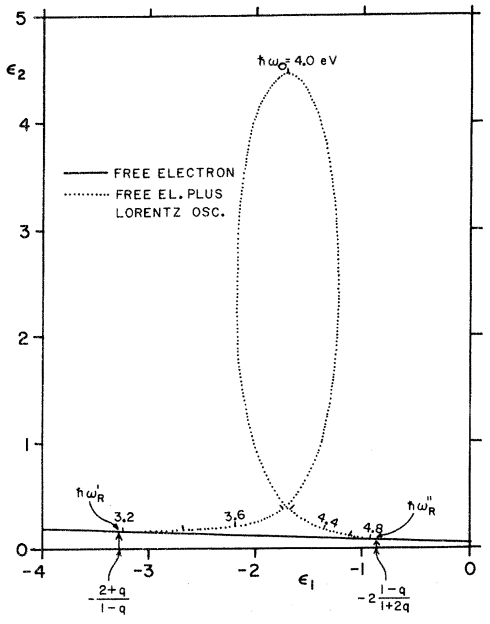

FIG. 3. Easy method of finding the OCR and plasma-resonance points on the $\tilde{\epsilon}(\omega)$ curve of a metal in aggregated form with parameter q is to draw the shortest vectors from the points indicated on the ϵ_1 axis to the curve. The particular curve drawn here for illustration is that used in Fig. 2 with $q = 0.7$, and with $\hbar\omega_0 = 4$ eV.

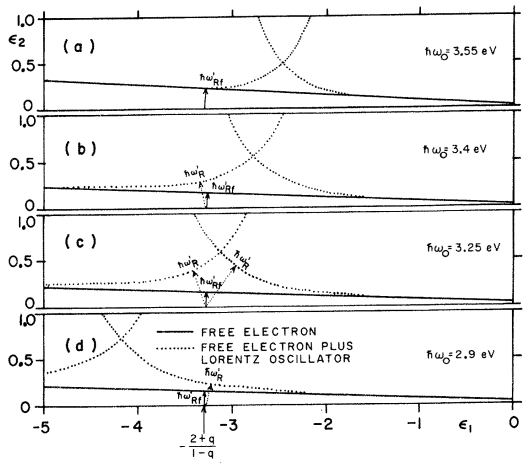

FIG. 4. Effect of the frequency position ω_0 of the interband transition in the free-electron $\tilde{\epsilon}(\omega)$ curve on the OCR of the aggregated system. The dotted vectors point to the shifted OCR frequency ω'_R and the solid vectors indicate the corresponding free-electron OCR positions ω'_{Rf}. Note the splitting of OCR in (c). The curves drawn here are identical with that in Fig. 3, except for the different values of ω_0 in the sequence (a)–(d).

Quantitatively, the aggregated dielectric function $\tilde{\xi}(\omega)$ may be obtained from Eq. (7) or from the graphical MG transformation used before.[4] Other optical functions such as the plasma-loss function, conductivity, and reflectance may be then calculated from $\tilde{\xi}(\omega)$.

In the following, we take a quantitative look at the effect of simulated interband transitions on the functions $\epsilon_1(\omega)$, $\epsilon_2(\omega)$, $\xi_1(\omega)$, $\xi_2(\omega)$, $L(\omega)$, and $R(\omega)$ of aggregated metal systems at $q = 0.7$ and $q = 0.2$, where the metal dielectric function is made up of free-electron and Lorentz-oscillator parts according to Eq. (19). The metal parameters are $\hbar\omega_{pf} = 6.6$ eV, $\tau = 2.6\times10^{-14}$ sec as before, $f = 0.05$, $\gamma^{-1} = 10^{-14}$ sec, and several values of $\hbar\omega_0$. In the calculations Eqs. (1), (19), and

$$R = \mathrm{Re}(\tilde{n} - 1)^2/\mathrm{Re}(\tilde{n} + 1)^2 \qquad (20)$$

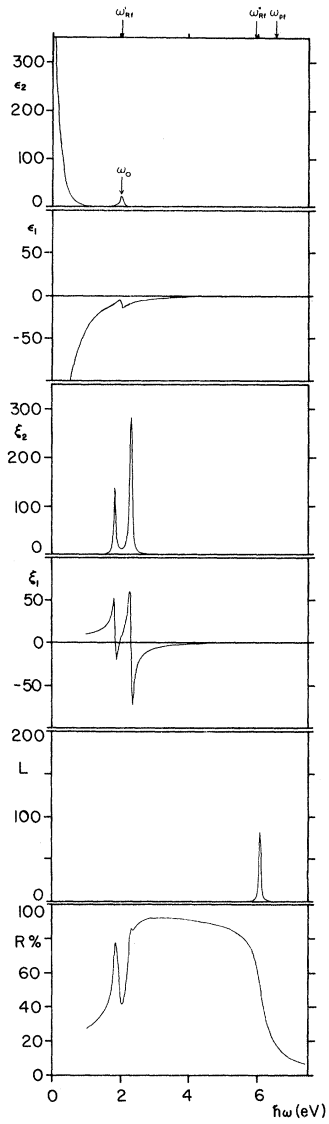

FIG. 5. Optical functions $\xi_2(\omega)$, $\xi_1(\omega)$, $L(\omega)$, and $R(\omega)$ of a $q=0.7$ aggregated system with metal dielectric function $\epsilon_2(\omega)$, and $\epsilon_1(\omega)$ containing a Lorentz oscillator at $\hbar\omega_0=2.04$ eV. This is close to the free-electron OCR frequency ω'_{Rf} and splitting of the OCR occurs. The OCR edge of the reflectivity is also split. The free-electron plasma peak is not effected.

were used, where $\tilde{n}^2=\tilde{\xi}$. Equation (20) gives the reflectivity at normal incidence.

The optical functions of interest for an aggregated system with $q=0.7$ are shown in Figs. 5 and 6 and those for $q=0.2$ are shown in Fig. 7. The effect of the Lorentz oscillator on the free-electron OCR, the loss function, and the relativity can be seen to be strong when ω_0 is near the free-electron OCR or the free-electron plasma frequency. It is also evident that the oscillator is "copied" from $\tilde{\epsilon}$ to $\tilde{\xi}$ by the MG transformation, with no significant frequency shift. The latter is an important property of the transformation and it can be used to identify interband peaks in the optical functions of aggregated metals.

The examples used above in Figs. 5 and 6 demonstrate quite clearly that there are four effects of the interband transitions in the metal particles on the optical functions of the aggregated system.

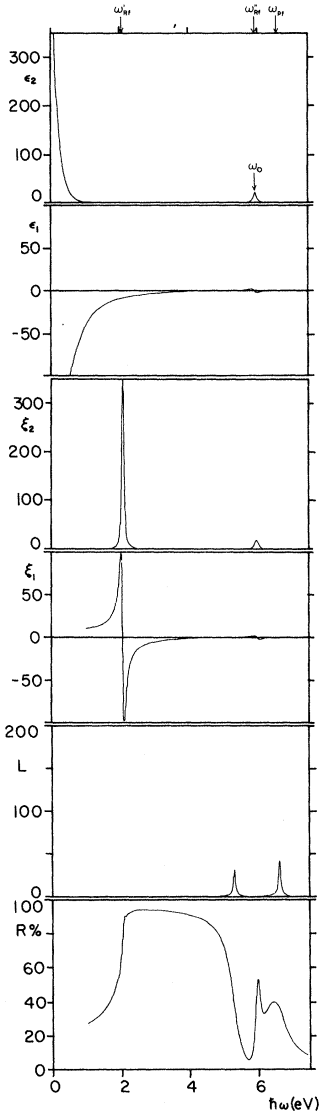

FIG. 6. Optical functions $\xi_2(\omega)$, $\xi_1(\omega)$, $L(\omega)$, and $R(\omega)$ of a $q=0.7$ aggregated system with metal dielectron function $\epsilon_2(\omega)$ and $\epsilon_1(\omega)$ containing a Lorentz oscillator at $\hbar\omega_0=6$ eV. This is close to the free-electron plasma peak ω''_{Rf} and splitting of the $L(\omega)$ peak occurs. The plasma edge of the reflectivity is also split. The OCR is not affected, but the interband peak is copied from ϵ_2 to ξ_2 and from ϵ_1 to ξ_1 by the MG transformation.

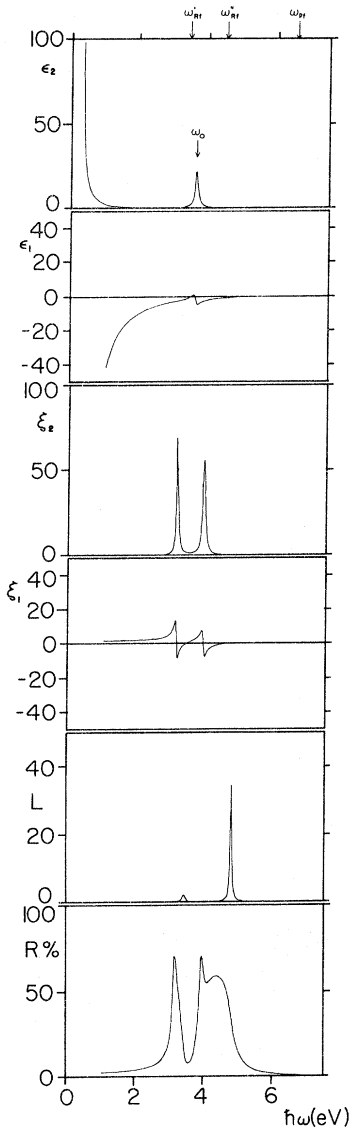

FIG. 7. Optical functions $\xi_2(\omega)$, $\xi_1(\omega)$, $L(\omega)$, and $R(\omega)$ of a $q=0.2$ aggregated system with metal dielectric function $\epsilon_2(\omega)$ and $\epsilon_1(\omega)$ containing a Lorentz oscillator at $\hbar\omega_0=3.6$ eV. This is close to both the free-electron OCR peak and the plasma peak and is seen to affect both. Splitting of the OCR occurs in $\xi_2(\omega)$ and shifting of the loss-function peak in $L(\omega)$ takes place. In the reflectivity curve, the OCR edge is split and the plasma edge is split. The higher OCR dip and the lower plasma dip coincide at 3.5 eV which causes the $R(\omega)$ curve to be double peaked.

They are (i) a splitting of the optical conduction resonance when the interband-transition frequency ω_0 is close to the free-electron OCR frequency ω'_{Rf}, (ii) a splitting of the loss function peak when the interband transition frequency ω_0 is close to the free-electron plasma frequency ω''_{Rf}, (iii) a shift of the OCR and loss-function frequencies when the interband-transition frequency approaches the free-electron OCR and plasma frequencies, respectively, and finally, (iv) a damping effect on the OCR and loss-function peaks when ω_0 is close to ω'_{Rf} and ω''_{Rf}, respectively. The direction of frequency shift of the OCR and loss-function peaks is to higher (lower) frequencies when the interband frequency approaches the OCR and loss function peaks from lower (higher) energies.

When the resonances are split into two peaks, one peak is always free-electron-like and the other is interbandlike. The nature of the peaks may be easily found using the property of the MG transformation mentioned above. The free-electron-like peak in the OCR or plasma-loss spectrum is found at different energies for different values of q, while the interbandlike peak of the doublet retains its position for all q values.

The reflectivity of the aggregated system at normal incidence also shows the effect of interband transitions. With no interband transitions present, the reflectivity is finite at frequencies between ω'_{Rf} and ω''_{Rf} and the $R(\omega)$ curve is smooth. With an interband transition present the frequencies ω'_R and ω''_R shift as discussed above and an absorption appears on the smooth $R(\omega)$ curve at the interband frequency ω_0. Moreover, if the interband component splits the loss function peak into two peaks, the reflectivity shows two onsets of transparency, one at each of the two loss-function peaks. In this case, the interband absorption shows up between the two plasma edges producing a double peak in the $R(\omega)$ curve at the high-energy side. This feature is readily seen in Fig. 6.

An inspection of Fig. 7 shows that as the aggregation parameter q is decreased, and as ω'_{Rf} and ω''_{Rf} move closer together, a Lorentzian oscillator placed between the two resonance frequencies may effect both the OCR and the loss function. This shows up quite dramatically in the reflectivity as it is seen from the figure. This effect arising in the low-q case comes about because as the loss function is split, the frequency of the lower plasma peak may coincide with that of the OCR peak. The latter may be interpreted when seen in experiments as the excitation of bulk-plasma resonance by light. However, this observed absorption is due either to the interband transitions or to the optical conduction resonance, and not to plasma resonance.

IV. REAL METALS

Some low-energy interband transitions (few eV) in certain metals resemble the Lorentzian oscilla-

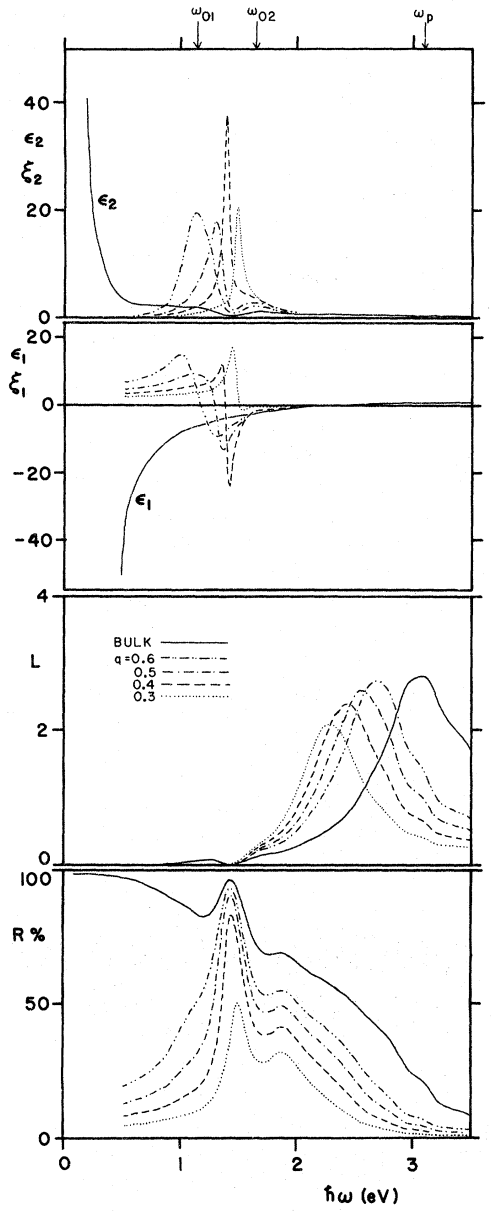

FIG. 8. Optical functions $\tilde{\epsilon}(\omega)$, $\tilde{\xi}(\omega)$, $L(\omega)$, and $R(\omega)$ of cesium bulk and aggregated metal with q values ranging from 0.3 to 0.6. Interband transitions at ω_{01} and ω_{02} affect the OCR, but not the free-electron plasma at ω_p.

tor used in our present treatment. The individual transitions are also spaced far enough apart in energy to be considered as independent oscillators, therefore the optical functions of these metals in bulk and aggregated form may be analyzed in terms of the results obtained here.

We chose the metals Cs, Ag, and Cu to illustrate the main points of the present work, namely the splitting, shifting, and damping of the plasma and OCR features of the metals by interband transitions. The dielectric functions for these metals were obtained from the work of Smith[7] and of Wang *et al.*[8] for Cs, from the work of Johnson and Christy[9] for Ag, and from the work of Ehrenreich and Philipp[10] for Cu. The optical functions $L(\omega)$ and $R(\omega)$ for the bulk, and the functions $\xi_1(\omega)$, $\xi_2(\omega)$, $L(\omega)$, and $R(\omega)$ for the aggregate were calculated from the bulk $\tilde{\epsilon}(\omega)$ data using Eqs. (1), (9),

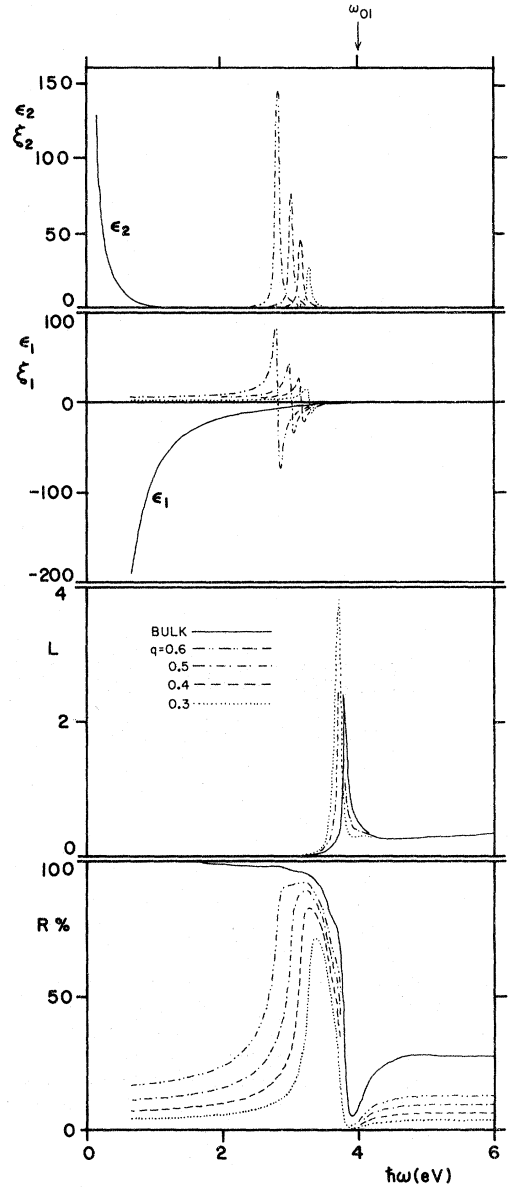

FIG. 9. Optical functions $\tilde{\epsilon}(\omega)$, $\tilde{\xi}(\omega)$, $L(\omega)$, and $R(\omega)$ of silver bulk and aggregated metal with q values ranging from 0.3 to 0.6. The main interband transition at ω_{01} does not affect the OCR, but it splits and shifts the free-electron plasma. The character of the peak in the loss function is interbandlike. Its free-electron-like twin is at a higher energy.

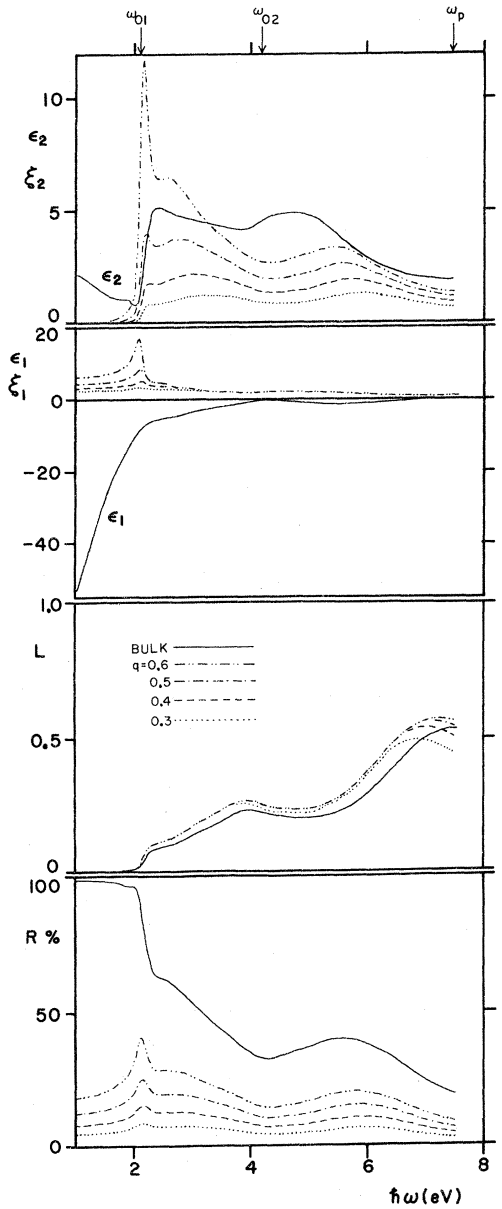

FIG. 10. Optical functions $\tilde{\epsilon}(\omega)$, $\tilde{\xi}(\omega)$, $L(\omega)$, and $R(\omega)$ of copper bulk and aggregated metal with q values ranging from 0.3 to 0.6. The lowest interband transition at ω_{01} splits and severely damps the OCR. The second interband transition at ω_{02} splits and shifts the free-electron plasma peak at ω_p. The two lower plasma peaks in the $L(\omega)$ spectra are interbandlike and the high one is free-electron-like.

and (20) at several values of the aggregation parameter q. The functions for the three metals are plotted in Figs. 8 (Cs), 9 (Ag), and 10 (Cu).

First we look at Cs in Fig. 8. This metal has two interband components in the low-energy range at approximately $\omega_{01} = 1.2$ eV and $\omega_{02} = 1.7$ eV. These are expected to affect the OCR, which lies in this general range. An inspection of the ξ_1 and ξ_2 curves in Fig. 8 show two effects. First, we see that ω_{01} damps the $q = 0.6$ and $q = 0.5$ OCR peaks which lie in its vicinity and that ω_{02} splits the OCR curves. At ω_{01} there is no splitting as this transition is very broad, but at ω_{02} the splitting is quite apparent from the ξ_2 plot for all but the $q = 0.3$ curve.

The same two interband components are also expected to show up as slight peaks in the loss-function curve with a q-independent position. This we see for all q curves in the $L(\omega)$ plot of Fig. 8. The reflectivity curves are equally effected at ω_{01} and ω_{02} for both the bulk metal and the aggregates. Moreover, the OCR edge (low-energy edge of the reflectivity curve) shows the damping effect at ω_{01} discussed above in the $q = 0.6$ and the $q = 0.5$ curves as slight humps. The splitting at ω_{02} in all the $R(\omega)$ curves is also evident.

The major peak of the loss function for Cs is seen from Fig. 8 to be approximately at 3.2 eV for the bulk. This value is lower than the calculated free-electron plasma resonance at $\hbar\omega_{pf} = 3.6$ eV. The reason for this, according to our present results, is the interband transition ω_{03} at 5.0 eV, which shifts ω_p from its free-electron value to 3.2 eV. The shifted plasma has nevertheless a free-electron-like character, which is indicated in the $L(\omega)$ plot by the orderly displacements of the various q curves from the bulk peak. The same orderly displacement in the reflectivity curves at the plasma edge also confirm the free-electron nature of the plasmon at ω_p.

Next, we analyze Ag in Fig. 9. The first interband transition of this metal is at $\omega_{01} = 4$ eV which is seen from the ξ_1 and ξ_2 curves to have no splitting or damping effect on the OCR at the particular q values considered. However the $q = 0.3$ OCR peak, lying closest to ω_{01}, is shifted slightly to a lower energy. The OCR edge in the $R(\omega)$ plot is found to be regular for each q value, and the various q curves are seen to be evenly spaced, except for the $q = 0.3$ OCR edge, which is shifted down slightly.

The major effect of the interband transition at ω_{01} for silver shows up in the loss function and in the $R(\omega)$ curve. The loss function peaks sharply at about 3.8 eV for the bulk and for all the aggregate curves, and similarly the $R(\omega)$ curve shows a plasma edge at this energy. The particular loss-function behavior for Ag is noteworthy for three reasons. First, the peak shown in Fig. 9 is at an energy far lower than that of the free-electron plasma $\hbar\omega_{pf} = 9.2$ eV. Secondly, the peak is at a lower energy than $\hbar\omega_{01}$ by 0.2 eV, and thirdly, the position of the peak is q independent. The

first feature may be explained in terms of the splitting of the free-electron plasma peak by a strong interband transition into an interbandlike part and a free-electron-like part, as shown by our results. In Fig. 9, we see the interbandlike peak, while the free-electron part lies at a higher energy. The downshift of the $L(\omega)$ peak from ω_{01} is the consequence of the splitting, which was shown in Fig. 6 to occur generally. The q independence serves to confirm that the loss-function peak is indeed the interband part because the MG transformation merely "copies" interband features from the bulk to the aggregated dielectric function while it shifts free-electron features in frequency with q, as it was discussed earlier. The crowding of the bulk and q curves at the plasma edge of the $R(\omega)$ curve also shows the q-independence effect.

One may find it puzzling that the next loss-function peak for Ag (not shown in Fig. 9) is at 7.5 eV, and not approximately 0.2 eV above $\hbar\omega_{pf}$ = 9.2 eV as one would expect from the present analysis. The reason for this is the presence of a strong interband transition at about $\hbar\omega_{02}$ = 16 eV, which splits and shifts the free-electron loss peak down to 7.5 eV and shifts the interbandlike peak up to about 18 eV. The result is a loss function with three peaks, two of which are interbandlike at 3.8 and 18 eV, and the third one which is free-electron-like at 7.5 eV.

Finally, we look at Cu in Fig. 10. The low-energy end of the spectrum contains two interband peaks, one at ω_{01} = 2.1 eV and the other at ω_{02} = 4.2 eV. The OCR of aggregated Cu lies in the vicinity of ω_{01}, therefore it is expected to be affected by the first interband transition. The effect is seen from the $\xi_1(\omega)$ and $\xi_2(\omega)$ curves in the figure to be substantial. The OCR peaks of all but the q = 0.3 curve are split as shown by the ξ_2 curves, and they are highly damped as shown by the ξ_1 curves. The strong damping also decreases the reflectivity of all aggregates, markedly. In fact the interband feature at ω_{01} is strong enough to cause a plasma edge to appear in the $R(\omega)$ curve at 2.1 eV.

The loss function in the figure is seen to contain peaks at 2.1 and 3.9 eV. These peaks are q independent, similar to the loss function peak of Ag, confirming their interbandlike character. The free-electron-like plasma peak appears at about 7.5 eV for the bulk and at lower energies for aggregates with decreasing q values. Here again, as for silver, we find that ω_{02} splits the free-electron plasma peak and shifts the interbandlike peak to about 0.2 eV below ω_{02}. However, the free-electron-like peak fails to be shifted up over ω_{pf} = 9.3 eV. Instead it is shifted down to 7.5 eV by a strong interband transition at ω_{03} = 13 eV again in a similar fashion to what was found for silver.

V. CONCLUSIONS

The effects of a single Lorentzian oscillator on the optical properties of a free-electron metal aggregate system were analyzed. Graphical and analytical examples were given using a hypothetical free-electron metal with a Lorentzian oscillator at q = 0.7 and 0.2, and it was found that the presence of the oscillator may shift or damp the free-electron OCR and plasma resonances, and it may split these resonances into a free-electron-like and an interbandlike doublet.

It was also found that the MG transformation of the bulk dielectric function $\tilde{\epsilon}(\omega)$ to the aggregate dielectric function $\tilde{\xi}(\omega)$ leaves the interband features unshifted in frequency, while the free-electron features, such as the OCR and the plasma peak, shift with q.

Finally, the optical functions of Cs, Ag, and Cu were analyzed at several q values in terms of the results obtained in this work and the various shifts, splittings, and dampings found in the dielectric function, loss function, and reflectivity spectra were identified. On the basis of qualitative success of the model, we conclude that the general features exhibited by the simple free-electron plus Lorentz oscillator system is typical of real metals; therefore, the results obtained here may be used in future work to improve the analysis of optical spectra of bulk and aggregated metals.

---

*Work supported by the National Research Council of Canada and by Welwyn Canada Ltd.

[1]J. C. Maxwell Garnett, Philos. Trans. R. Soc. Lond. 203, 385 (1904); A205, 237 (1906).
[2]E. C. Chan and J. P. Marton, J. Appl. Phys. 45, 5004 (1974).
[3]J. P. Marton and E. C. Chan, J. Appl. Phys. 45, 5008 (1974).
[4]J. P. Marton and J. R. Lemon, Phys. Rev. B 4, 271 (1971).
[5]J. P. Marton and J. R. Lemon, J. Appl. Phys. 44, 3953 (1973).
[6]See, for example, H. Ehrenreich and H. R. Philipp, Phys. Rev. 128, 1622 (1962), for bulk Ag.
[7]N. J. Smith, Phys. Rev. B 2, 2840 (1970).
[8]U. S. Wang, E. T. Arakawa, and T. A. Callcott, J. Opt. Soc. Am. 61, 740 (1971).
[9]P. B. Johnson and R. W. Christy, Phys. Rev. B 6, 4320 (1972).
[10]H. Ehrenreich and H. R. Philipp, Phys. Rev. 128, 1622 (1962), and (private communications).